

STRUCTURAL AND RESIDUAL STRESS ANALYSIS BY X-RAY DIFFRACTION ON POLYMERIC MATERIALS AND COMPOSITES

Viktor Hauk

Institut für Werkstoffkunde, RWTH Aachen,
D-52056 Aachen, Germany

HISTORICAL REVIEW

Two papers are mentioned [1], [2] which describe basic tests on polymeric materials. Also a lot of publications of Sakurada et al. dealing with the Young´s modulus of polymeric materials are known. But the history of systematic stress analysis by X-ray diffraction starts with papers of Barrett and Predecki [3]. Fig. 1 tells the progress of the development in the studies on polymeric materials and composites. Here and subsequently, a distinction will be made between amorphous and semicrystalline polymers. Small particles are used to get a crystalline phase for strain measurement. Besides this filler of small amount, reinforcing fibers of higher amount are used to increase the strength of the polymers.

Results of different research groups have contributed to the present state of the art. The items listed in Fig. 1 refer to the very first paper on the specific branch of research. For example, the author's group has studied besides the first paper (1982) [4] primarily the correlation of manufacturing and structural parameters with the residual stresses (RS) 1989 [5], the micro RS 1991 [6], the structural and the residual stresses and the RS profiles in reinforced polymeric components 1995 [7].

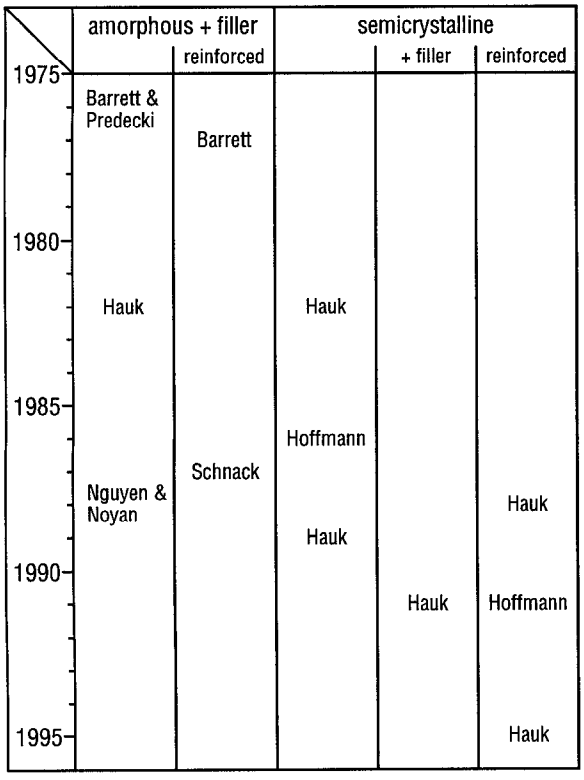

Fig. 1: A historical review of the first papers of each branch of research work on polymeric materials and composites.

POLYMERS

The polymers, amorphous, semicrystalline, amorphous + filler and the semicrystalline polymers + reinforcing fibers are listed in Table 1. References are made to the materials when describing the test results. Most of the results are concerned with injection molded plates.

Table 1: Semicrystalline and amorphous polymers and polymeric composites dealt with in different papers.

polymer	crystallinity α, β vol. %	amorphous vol. %	crystal structure
Polyethylene (PE)	70	30	orthorhombic
Polypropylene (PP)	α: 45 β: 10	45	monoclinic
Polybutyleneterephathalate (PBT)	30	70	triclinic
Polyetheretherketone (PEEK)	30	70	orthorhombic
Polyetherketone (PEK)	30	70	orthorhombic
Polyamide (PA-6)	35	65	monoclinic
Polystyrene (PS) High impact Polystyrene (HI-PS)	0	100	Al : fcc
Epoxy / C-Laminate	0	100	Nb : bcc CdO : fcc
PMMA	0	100	Ag : fcc

polymer	phase		filler reinforcement
	measurable, crystallinity	not measurable	
PP	α-PP, 45 vol.%	amorphous, 45vol.% β-PP, 10 vol.%	4 vol.% Al-powder 1 vol.% Cu-powder
PBT	PBT, 30 vol.%	amorphous, 70vol.%	22 vol.% glass spheres 21 vol.% glass fibers
PEK	PEK, 30 vol.%	amorphous, 70vol.%	15 vol.% C- fibers 18 vol.% glass fibers

MEASUREMENT

Strain measurements and stress evaluation on polymers are in many respects different from those of studies of RS in metals and ceramics. The different parameters are listed in Table 2. The main points are: suitable peaks are found only in the front reflection zone, large X-ray elastic constants (XEC), lattice distance strongly dependent on temperature, large penetration depth of X-rays, and

the measurement can be made in reflection and in transmission. Although the texture of crystallites is strong and the exact determination of the peaks is difficult, linear lattice strain dependences are observed. An example is shown in Fig. 2 [8].

The symbols used are shown in Fig. 3. Also the basic formulae are given. For experts, further explanations are not necessary [9]. Table 3 summarizes the possibilities to determine the macro- and microstresses for the three categories of polymers: amorphous + filler, semicrystalline + filler and semicrystalline + fibers. More details of the definition of stresses, the transfer factor and of the compensation of macro- and microstresses can be found in [9].

Table 2: Comparison of the X-ray analysis on polymers or metals.

	Metals	Amorphous polymers + crystalline fillers	Semicrystalline polymers
Structure	cubic, hexagonal, tetragonal	amorphous	triclinic, monoclinic, rhombic
Suitable peaks	back-reflection-zone	back-reflection-zone for metal-fillers	front-reflection-zone
Young's modulus	large	small	small
X-ray elastic constant (XEC)	small	factor 2 for metal-fillers	large
Lattice parameter			strong dependence on temperature
Texture	dependence on processing and mechanical treatment		strong dependence on processing
Reinforcement	strength improvement by whiskers	less strength improvement by fillers	high strength improvement by fibers
XEC calculation	for all crystal symmetries using monocrystal coefficients	for all crystal symmetries of metal-fillers using monocrystal coefficients	only for PE using monocrystal coefficients, other polymers using macroelastic coefficients
Penetration depth	low	large	large
Calibration	no correction for penetration depth	correction for large penetration depth	correction for large penetration depth
Measuring technique	reflection	reflection	reflection and transmission
Diffractometer	Ψ-, Ω-diffractometer	Ψ-, Ω-diffractometer for metal fillers	Ψ- for reflection technique, Ω- for transmission technique
Microstresses	between phases	in embedded fillers	between polymer and reinforcement

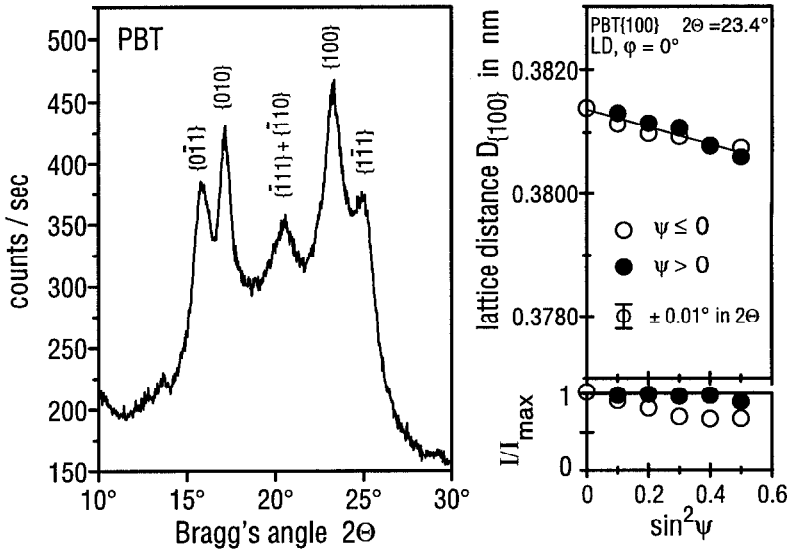

Fig. 2: Debyeogram and lattice distant $D_{\{100\}}$ versus $\sin^2\psi$ of PBT [8].

$$\sigma_{ik} = 0$$

$$\varepsilon_{\varphi,\psi} = \tfrac{1}{2}s_2\left(\sigma_1\cos^2\varphi\sin^2\psi + \sigma_2\sin^2\varphi\sin^2\psi + \sigma_3\cos^2\psi\right) + s_1\left(\sigma_1+\sigma_2+\sigma_3\right)$$

$$\sigma_1 - \sigma_3 = \frac{1}{\frac{1}{2}s_2}\frac{1}{D_0}\frac{\partial D_{\varphi=0,\psi}}{\partial \sin^2\psi}$$

$$\sigma_2 - \sigma_3 = \frac{1}{\frac{1}{2}s_2}\frac{1}{D_0}\frac{\partial D_{\varphi=90,\psi}}{\partial \sin^2\psi}$$

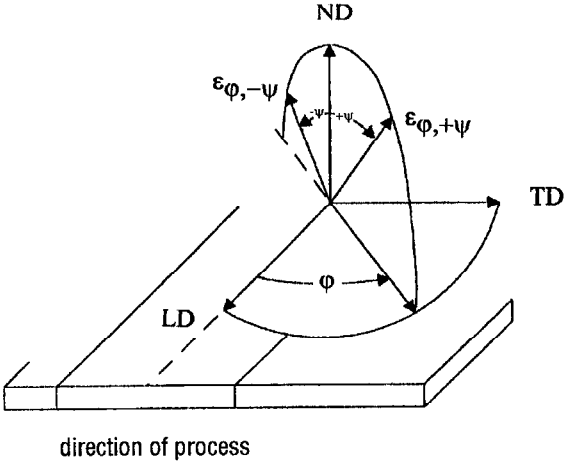

$$\sigma_3 = \frac{\frac{D_{\varphi=0,\psi=0} - D_0}{D_0} - s_1(\sigma_1+\sigma_2)}{s_1 + \frac{1}{2}s_2}$$

$$= \frac{1}{D_0\left(3s_1 + \frac{1}{2}s_2\right)}\left(D_{\varphi=0,\psi=0} - D_0 - \frac{s_1}{\frac{1}{2}s_2}\left(\frac{\partial D_{\varphi=0,\psi}}{\partial \sin^2\psi} + \frac{\partial D_{\varphi=90,\psi}}{\partial \sin^2\psi}\right)\right)$$

stress free direction $\quad \frac{1}{2}\left(\varepsilon_{+\psi} + \varepsilon_{-\psi}\right) = 0 \qquad \sigma_i$ independent direction $\quad \frac{\partial\left(\varepsilon_{+\psi} + \varepsilon_{-\psi}\right)}{\partial\,\sigma_i} = 0$

$$\text{phase stress} = \underset{\text{macro (m)}}{\sigma^{L}} + \sigma^{I} + \underset{\text{micro}}{\sigma^{II}_{\text{m - dep.}}} + \sigma^{II}_{\text{m - indep.}} \text{ (thermal, process)}$$

Fig. 3: Symbols and formulae to calculate stresses from X-ray diffraction results [9].

Table 3: Formulae to evaluate macro and micro RS on polymeric materials and composites, n. d.: not determinable
×: stress compensation using volume ratio [9].

phase / stress		amorphous	filler	semicrystalline	filler	semicrystalline	reinforcement
$\sigma^{I}_{mech.}$		•		•		•	
$\overline{\sigma}^{\alpha}$			$\langle \sigma^{L} + \sigma^{I} + \sigma^{II} \rangle^{f}$	$\langle \sigma^{L} + \sigma^{I} + \sigma^{II} \rangle^{\alpha'}$	$\langle \sigma^{L} + \sigma^{I} + \sigma^{II} \rangle^{f}$	$\langle \sigma^{L} + \sigma^{I} + \sigma^{II} \rangle^{\alpha'}$	
σ^{I}_{x}		n.d.		•		n.d.	
σ^{L}		n.d.	$\overline{\sigma}^{\alpha} - \sigma^{I} - \langle \sigma^{II} \rangle^{f}$	•		$\overline{\sigma}^{\alpha'} - \sigma^{I} - \langle \sigma^{II} \rangle^{\alpha'}$	n.d.
micro RS	total	×	$\langle \sigma^{I} + \sigma^{II} \rangle^{f} - \sigma^{I}$	$\langle \sigma^{I} + \sigma^{II} \rangle^{\alpha'} - \sigma^{I}$	$\langle \sigma^{I} + \sigma^{II} \rangle^{f} - \sigma^{I}$	$\langle \sigma^{I} + \sigma^{II} \rangle^{\alpha'} - \sigma^{I}$	×
micro RS	$\sigma^{II}_{m-dep.}$	×	$(f^{f} - 1)\sigma^{I}$	$(f^{\alpha'} - 1)\sigma^{I}$	$(f^{f} - 1)\sigma^{I}$	$(f^{\alpha'} - 1)\sigma^{I}$	×
micro RS	$\sigma^{II}_{m-indep.}$	×	$\langle \sigma^{I} + \sigma^{II} \rangle^{f} - f^{f}\sigma^{I}$	$\langle \sigma^{I} + \sigma^{II} \rangle^{\alpha'} - f^{\alpha'}\sigma^{I}$	$\langle \sigma^{I} + \sigma^{II} \rangle^{f} - f^{f}\sigma^{I}$	$\langle \sigma^{I} + \sigma^{II} \rangle^{\alpha'} - f^{\alpha'}\sigma^{I}$	×

• experimentally determinable

$\overline{\sigma}^{\alpha}$ phase stress σ^{L} load stress σ^{I} macrostress σ^{II} microstress

f stress transfer factor index f filler index α' crystalline + amorphous phase

The X-ray elastic constants (XEC) s_1 and $½s_2$ must be evaluated experimentally except for PE for which the compliances of the monocrystal are known. In Fig. 4 the results of calculations and of tests are shown [10]. The XEC $(s_1 + ½s_2)^{-1} = E^X$ are plotted versus the macro Young's modulus.

Of special interest is the comparison of calculated XEC (models of crystallite coupling of Voigt, Reuss, Eshelby-Kröner) and those evaluated experimentally in the direction of the chains and perpendicular to them. A thorough look reveals that the best correlation between calculation and experiment is that using the Eshelby-Kröner model of an anisotropic ellipsoidal crystallite in an isotropic matrix.

A special topic is the study of a spherical particle within a matrix. Fig. 5 shows the result of the calculations of [11] and of [12]. One can notice that a Poisson's ratio in the usual range 0.2 to 0.4 has a negligible influence. As a consequence, an inclusion of a metallic particle within a polymeric matrix gets two times the macrostress in the stress direction and minus 0.3 times that in the transverse direction.

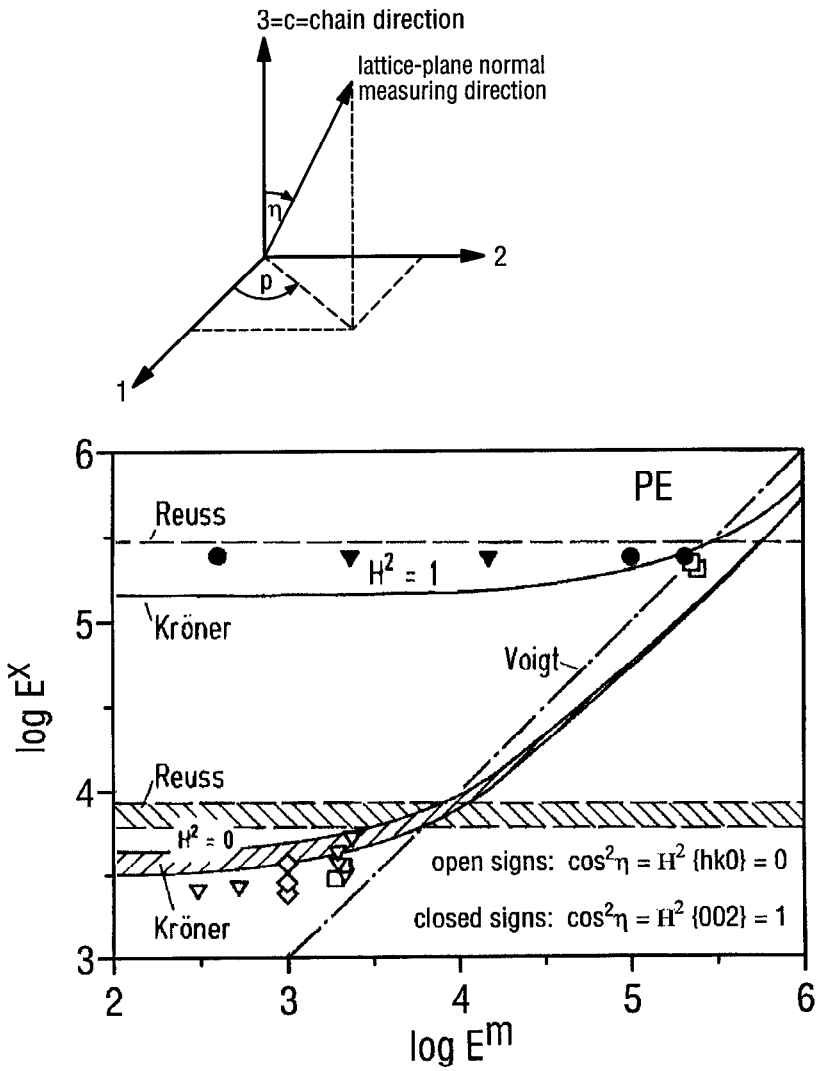

Fig. 4: $E^X = (s_1 + ½s_2)^{-1}$ versus E^{macro} of PE longitudinal and transverse to the chain direction. Calculated values according to the models of crystallite coupling by Voigt, Reuss, Eshelby-Kröner [10].

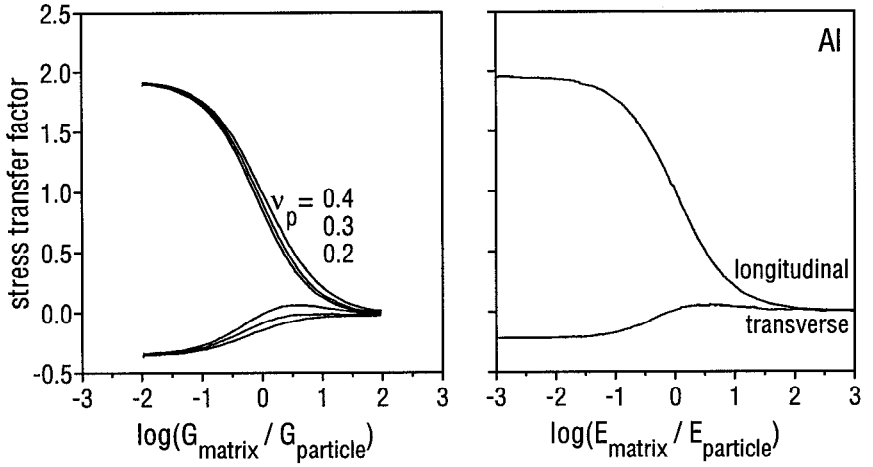

Fig. 5: Stress transfer factor versus the ratio macroelastic constants of matrix and embedded particle calculated by [11] for Poisson's ratio 0.2, 0.3, 0.4 and by [12] for Al.

RESULTS

Amorphous polymers. Fig. 6 shows the stress in Al particles (10 m.% = 4.1 vol. %) versus the applied stress in the load and in the transverse direction [13]. The transfer factors of about 2 and -0.3 are well verified. The curve for the stress direction shows some evidence for debonding at the particle - matrix interface. The correlation between the X-ray RS and the mechanically determined macro RS for Al particles in the HI-PS matrix is plotted in Fig. 7 [14]. There exist micro RS in the Al particles.

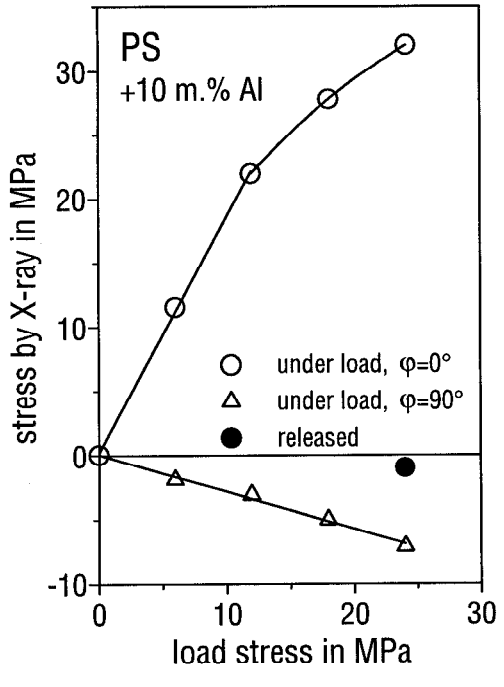

Fig. 6: Stress in load and transverse direction determined on the Al particles versus the load stress [13].

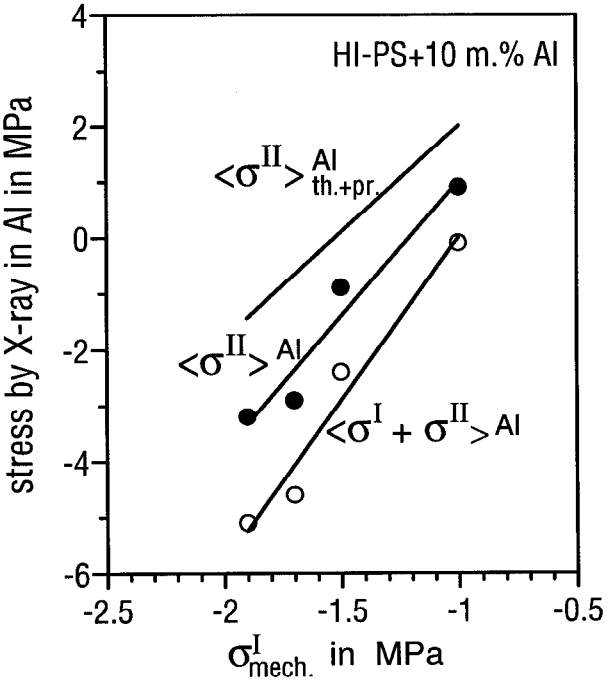

Fig. 7: Macro and micro RS of Al particles versus the mechanically determined macro RS in HI-PS injection molded plates [14].

Systematic studies on epoxy+C fibers laminates were made by Schnack et al. [15], [16]. Powders of Nb or CdO were inserted between the first and the second unidirectional reinforced ply. Results on different laminates are shown in Fig. 8 and Fig. 9. The stacking series are noted. An evaluation assuming a triaxial stress state results in linear dependences versus the applied load and at the edges shows evidence of shear stresses.

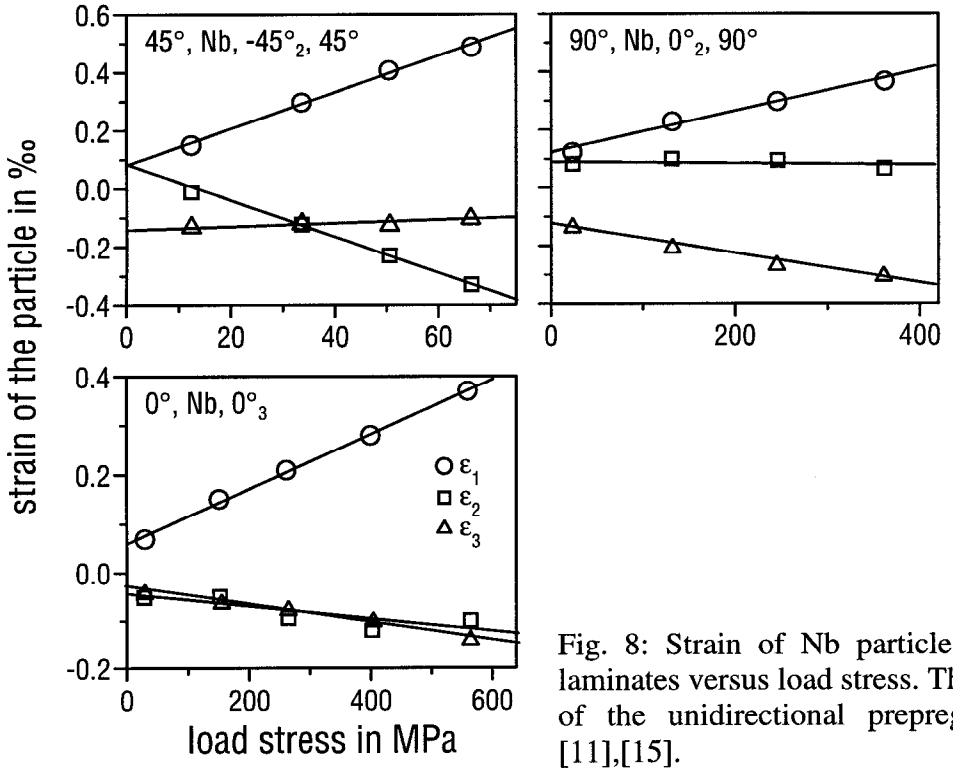

Fig. 8: Strain of Nb particles in different laminates versus load stress. The stacking up of the unidirectional prepregs are noted [11],[15].

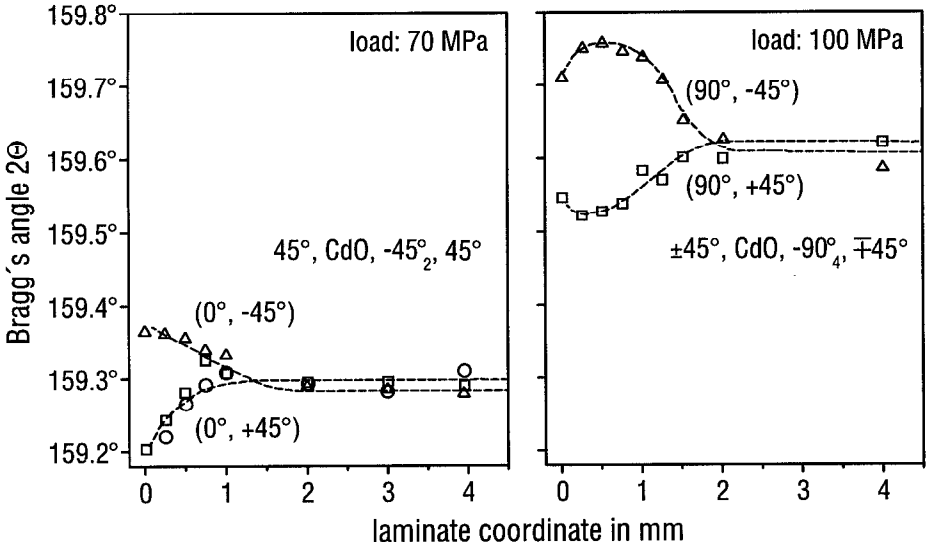

Fig. 9: Shears on the end of laminates, the measurement parameters (φ,ψ) and the stacking series of the plies are given [16].

Semicrystalline polymers. Fig. 10 shows the comparison of stress profiles evaluated by the mechanical deflection method and by the X-ray transmission technique [17]. The surface stresses determined by the X-ray reflection method fit very well to the results of the transmission technique. In Fig. 11 is plotted the test result of X-ray versus the load stress [8]. At higher stresses the amorphous phase does flow, the crystalline phase takes more stress and RS are the consequence.

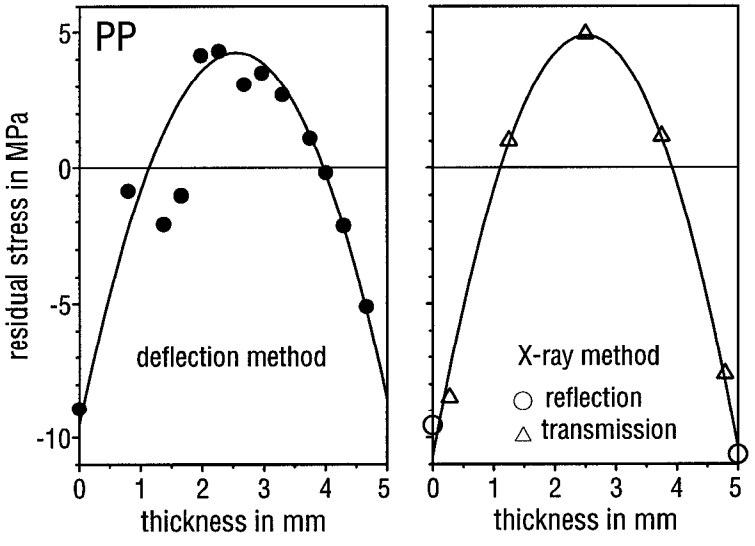

Fig. 10: RS profile of a PP injection molded plate determined by a mechanical method (left) and by X-ray method (right) [17].

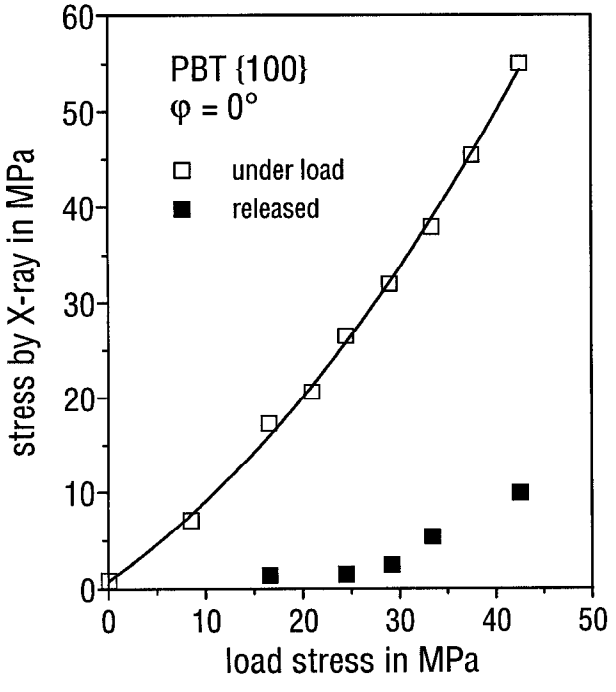

Fig. 11: RS versus load stress in the manufacturing direction under load and after releasing the load [8].

Results of measurement on the crystalline phase of semicrystalline PP and on the Al particles are plotted in Fig. 12 [5]. Again the stresses in the Al powder are twice of those in the matrix in the longitudinal and -0.3 in the transverse direction, respectively. The stresses in the crystalline phase correlate with the load stress. At higher applied stresses the Al particles start to flow.

When there are RS in the Al particles it is impossible to determine the macro RS by measurements of the strain in the particles. Fig. 13 [17] demonstrates the results on a PP matrix with Al or Cu particles. Measurements of the strain in the crystalline phase represent the macro RS. In the particles there are micro RS, too.

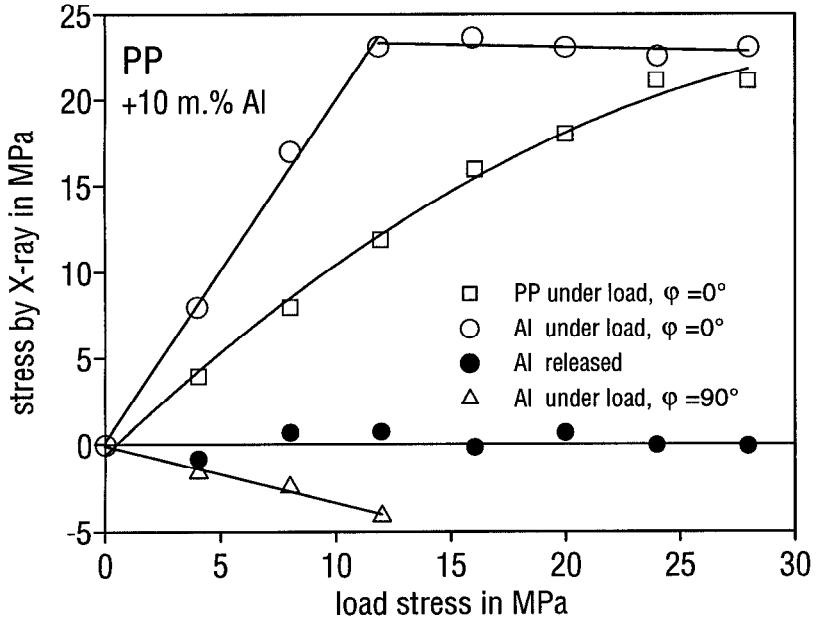

Fig. 12: RS versus load stress in a semicrystalline PP + 10 m.% (3.6 vol.%) Al injection molded plate [5].

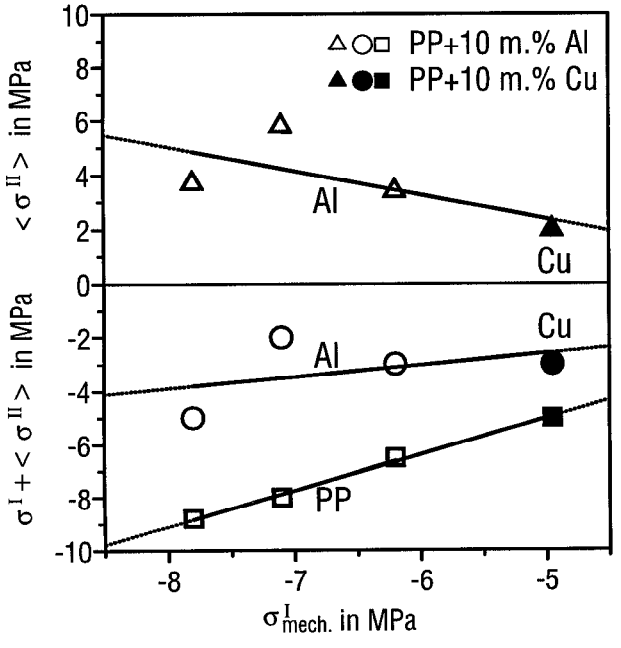

Fig. 13: Micro (top) and micro plus macro (bottom) RS versus macro RS in semi-crystalline PP + 10 m.% Al or Cu (3.6 or 1.1 vol.%)[17].

Reinforced semicrystalline polymers. Fig. 14 [18] and Fig. 15 [7] show evaluations of the triaxial RS state versus the load stress. The polymers and the fibers are specified. In the pure polymers the stress state is uniaxial. The reinforcements result in a triaxial stress state and the effect of the fibers can be clearly observed. The relative stress in the load direction is only a small part of the applied stress.

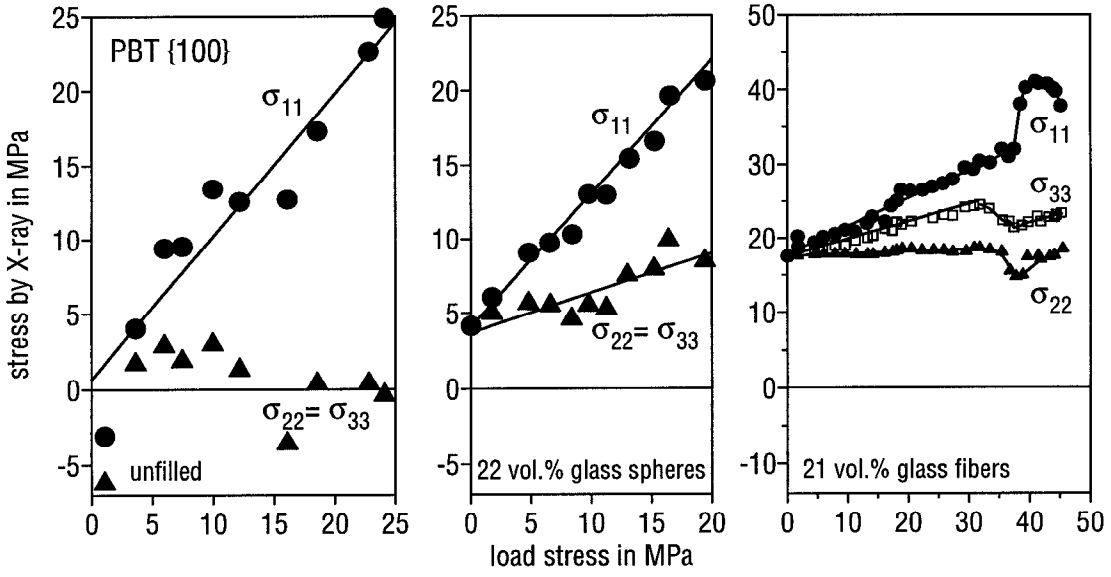

Fig. 14: Triaxial study of stress determined by X-ray versus load stress of PBT without and with glass reinforcement [18].

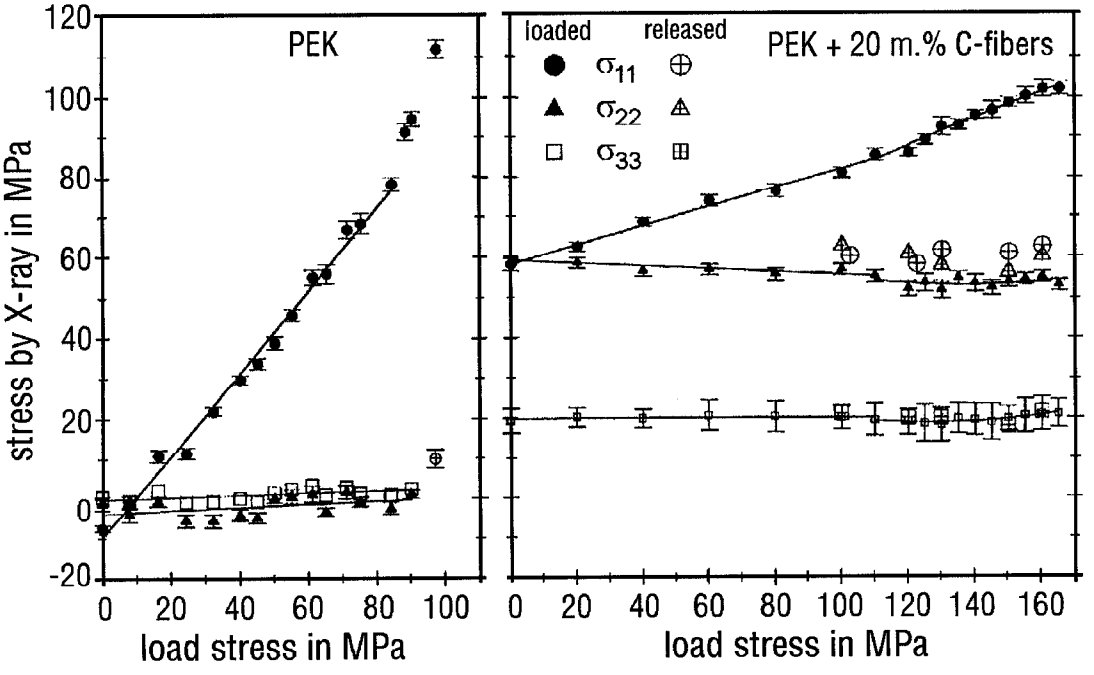

Fig. 15: Study of triaxial stresses determined by X-rays versus load stress of pure PEK and PEK reinforced by 20 m.% (15 vol.%) C fibers [7].

The stress profiles in C- and glass-fibers-reinforced PEK were studied by mechanical and X-ray methods [19], [20]. Since only the strains in the crystalline phase of the polymer and not of the fibers can be measured the macro RS-profile must be determined by the deflection method.

The X-ray evaluation gives the macro plus the micro RS. The mechanical method needs several specimens which have been thinned down from one side. The X-ray method uses one specimen with stepwise surface-layer removal from both sides to avoid deflection. Fig. 16 and Fig. 17 show the procedure and the results. The macrostress distribution was symmetrizised (left) and transformed to the state after both side removal (center). The determined macro + micro RS-profile was transformed to the real RS state. The micro RS profile was evaluated by subtracting the macro RS from the macro + micro RS-profile (center) under the assumption that the micro RS do not relax by the removal process (right). As a check of the procedure the macro RS (left) plus the micro RS (right) should give the actual macro plus micro RS (center).

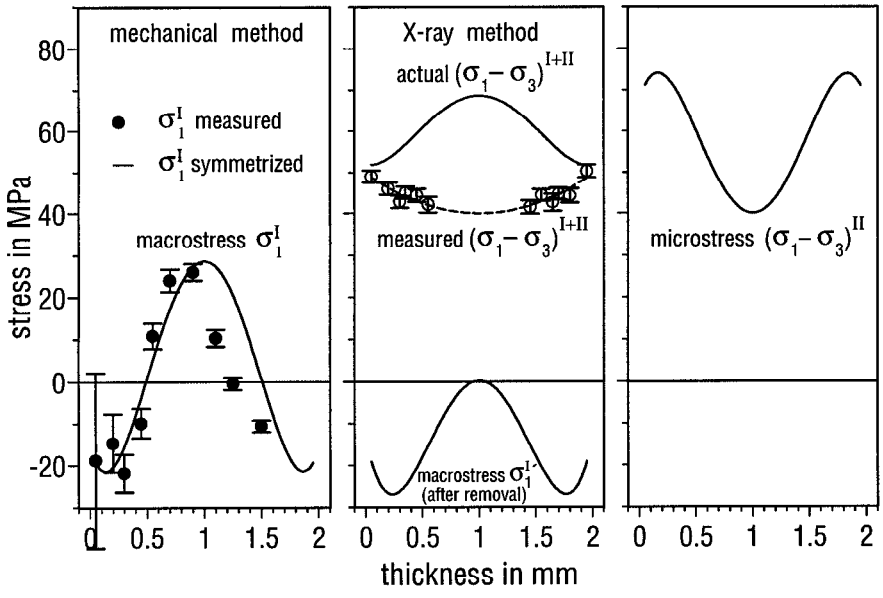

Fig. 16:
Macro and micro RS-profiles in PEK + 20 m.% (15 vol.%) C fibers [19].

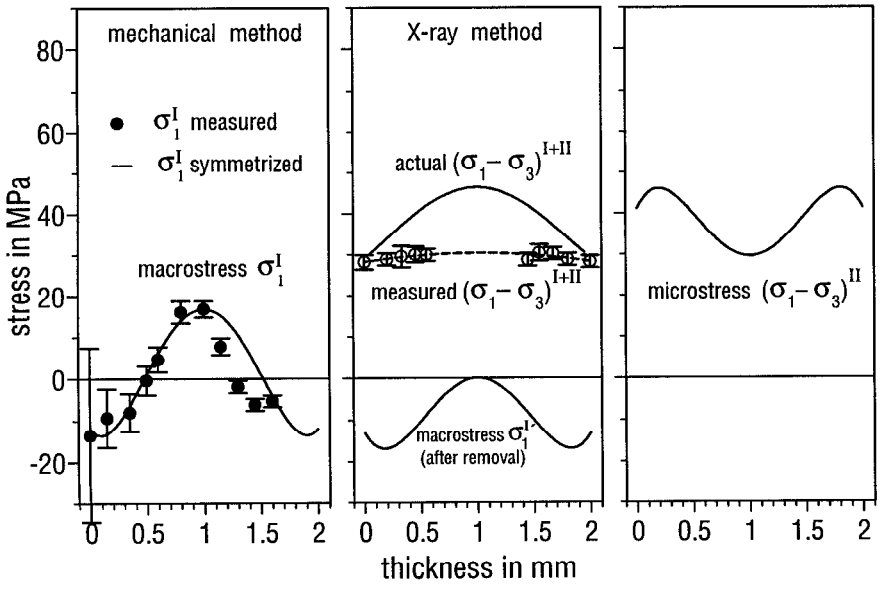

Fig. 17:
Macro and micro RS-profiles in PEK +30 m.% (18 vol.%) glass fibers [20].

Special polymers are developed for use at elevated temperatures. Injection molded plates of pure and C reinforced PEK were tested for stability of their RS state [19]. Each small specimen cut from the plate was tempered 2 hours at different elevated temperatures. The RS state was determined at room temperature on the surface of the small plate. The results are shown in Fig. 18. The pure PEK (left, bottom) shows nearly a stress free state, but the value of the stress free lattice spacing is drastically altered with the temperature (right). This D_0 versus temperature profile was used to evaluate the σ_{33} component. Specimens of PEK + 20 m.% C fibers show a triaxial RS state as expected, the surface RS components (left, top), decrease slightly with the temperature. A pronounced decrease of the RS component in the thickness direction begins at 200°C. Such results help to understand the stability or the relaxation of the materials characterists at elevated temperatures.

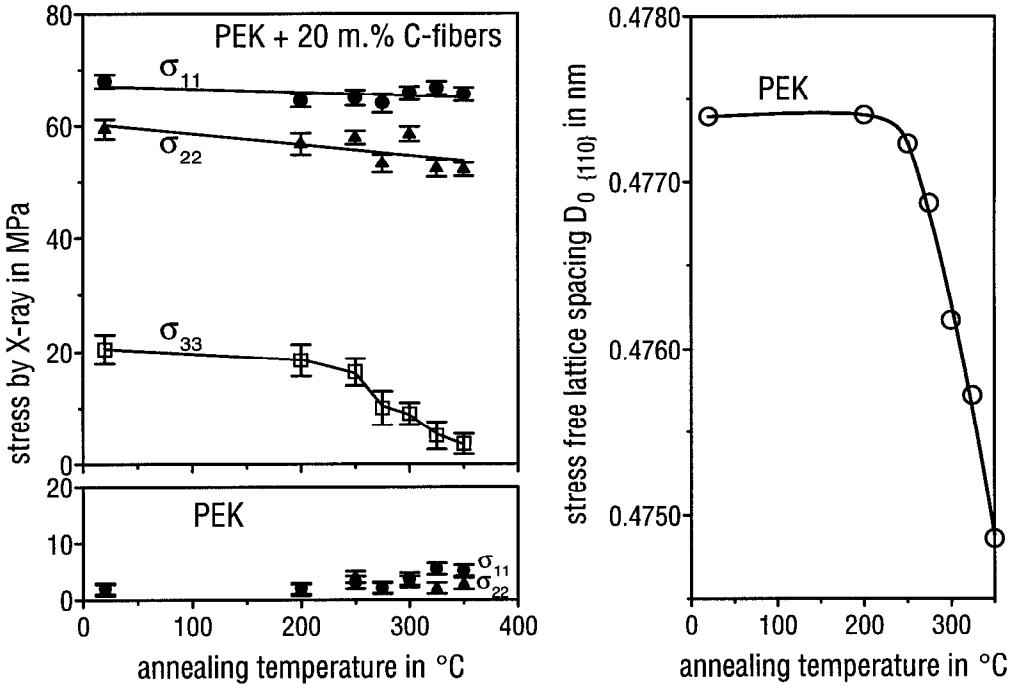

Fig. 18: RS state (bottom, left) and lattice spacing (right) of the pure PEK as well as the triaxial RS state of PEK + 20 m.% (18 vol.%) C fibers (left, bottom) versus annealing temperature. Each specimen of injection molded plates was 2 hours tempered at the specific temperature [19].

CONCLUSION AND SUMMARY

Table 4 summarizes the results of RS studies on injection molded plates. Shown are the macro and micro RS on the surface. The signs minus and plus indicate observed compressive and tensile RS. RS marked with × have been calculated from the balance of stresses using the volume fraction. Of practical interest are the results on reinforced semicrystalline polymers. As indicated, the thermal RS can be calculated using Eshelby´s theory.

The next step should be research work with reinforced composites in which the stresses in both phases, the crystalline one and the fibers, can be determined. Such tests using high modulus C fibers with a strong {002} peak are underway.

Table 4: Macro and micro RS in different injection molded plates of polymeric materials and composites, qualitatively.

– compression, + tension, X stress compensation using volume ratio, XX calculated

phase / stress		amorph. + filler		semicryst. + filler		semicryst. + reinf.	
		HI-PS	Al powder	PP	Al powder Cu	PEK	C fiber glass
$\sigma^{I}_{mech.}$		–		–		–	
$\overline{\sigma}^{\alpha}$			–	–	–	+	
σ^{I}_{X}				–			
micro RS	total	≈ 0 $+^{X}$	–	≈ 0 –	+	+	$-^{X}$
	$\sigma^{II}_{m\text{-}dep.}$	≈ 0 $+^{X}$	–	≈ 0 +	–	+	$-^{X}$
	$\sigma^{II}_{m\text{-}indep.}$	≈ 0 $+^{X}$	–	≈ 0 –	+	+	$-^{X}$
	thermal process					$+^{XX}$	$-^{XX}$

ACKNOWLEDGEMENT

The Deutsche Forschungsgemeinschaft, Bonn, has thankfully sponsored the activities of the following members of the authors group: Dr. G. Vaessen, Dr. D. Ley, Dr. H. Behnken, Dipl.-Ing. D. Chauhan.

REFERENCES

[1] I. Sakurada, Y. Nukushina, T. Ito, J. Polymer Sci., **57** (1962) 651-660

[2] S. I. Kontorovich, K. A. Lavrova, V. V. Davidov, G. M. Plavnik, E. D. Shukin, Strukt. Svoistva Proverkh, Sloev. Polim., (1972) 143-147

[3] C. S. Barrett, P. Predecki, Polym. Eng. Sci., **16** (1976) 602-608
C. S. Barrett, Adv. X-Ray Anal., 20 (1977) 329-336

[4] V. Hauk, A. Troost, G. Vaessen, Materialprüf., **24** (1982) 328-329

[5] V. Hauk, A. Troost, D. Ley, "Nondestructive Characterization of Materials"; Eds. P. Höller, V. Hauk, G. Dobmann, C. O. Ruud, R. E. Green, Springer Verlag Berlin, Heidelberg a.o., (1989) 207-214

[6] H. Behnken, D. Chauhan, V. Hauk, Mat.-wiss. u. Werkstofftech., **22** (1991) 321-331

[7] D. Chauhan, V. Hauk, VDI Berichte, **1131** (1995) 533-536

[8] D. Chauhan, V. Hauk, Mat. wiss. u. Werkstofftech., **23** (1992) 309-315

[9] V. Hauk, "Structural and Residual Stress Analysis by Nondestructive Methods", Elsevier, Amsterdam, Lausanne, New York, a.o., (1997)

[10] H. Behnken, V. Hauk, Mat.-wiss. u. Werkstofftech., **24** (1993) 356-361

[11] M. Wörtler, Doctorate thesis, Universität Karlsruhe (TH), (1988)

M. Wörtler, VDI-Verlag Düsseldorf, Fortschritt-Berichte VDI, Reihe 1, **169** (1989).

[12] H. Behnken, Doctorate thesis, RWTH Aachen, (1992)

[13] D. Ley, Doctorate thesis, RWTH Aachen, (1988)

[14] D. Chauhan, V. Hauk, Internal report, (1991)

[15] M. Wörtler, E. Schnack, VDI-Berichte, **631** (1987) 163-174

[16] B. Prinz, R. Meyer, E. Schnack, "Residual Stresses"; Eds. V. Hauk, H. P. Hougardy, E. Macherauch, H.-D. Tietz, DGM Informationsgesellschaft Verlag, Oberursel, (1993) 623-632
B. Prinz, E. Schnack, J. Comp. Mat., **31** (1997) 852-873

[17] H. Behnken, D. Chauhan, V. Hauk, Mat.-wiss. u. Werkstofftech., **22** (1991) 321-331 supplemented by the Cu results

[18] H. Hoffmann, H. Kausche, Ch. Walther, R. Androsch, Mat.-wiss. u. Werkstofftech., **22** (1991) 427-433
H. Hoffmann, Ch. Walther, "Residual Stresses"; Eds. V. Hauk, H. P. Hougardy, E. Macherauch, H.-D. Tietz, DGM Informationsgesellschaft Verlag, Oberursel, (1993) 613-623

[19] D. Chauhan, V. Hauk, "Proc. Fourth European Conference on Residual Stresses, ECRS 4"; Eds. S. Denis, J. L. Lebrun, B. Bourniquel, M. Barral, J.-F. Flavenot, Cluny (1996) 891-900

[20] D. Chauhan, V. Hauk, "The Fifth International Conference on Residual Stresses, ICRS-5"; Eds. T. Ericsson, M. Oden, A. Andersson, Linköpings Universitet, (1997) 892-897